tools will be of utmost importance for safe genome modification and perhaps for gene therapy. Potential avenues for improving CRISPR specificity include evaluating Cas9 homologs identified through bioinformatics and directed evolution of these nucleases toward higher specificity. Similarly, the range of CRISPR-targetable sequences could be expanded through the use of homologs with different PAM requirements (*9*) or by directed evolution. Finally, inactivating one of the Cas9 nuclease domains increases the ratio of HR to NHEJ and may reduce toxicity (figs. S1A and fig. S3) (*4*, *5*), whereas inactivating both domains may enable Cas9 to function as a retargetable DNA binding protein. As we explore these areas, we note that another parallel study (*21*) has independently confirmed the high efficiency of CRISPR-mediated gene targeting in mammalian cell lines. We expect that RNA-guided genome targeting will have broad implications for synthetic biology (*22*, *23*), the direct and multiplexed perturbation of gene networks (*13*, *24*), and targeted ex vivo (*25*–*27*) and in vivo gene therapy (*28*).

References and Notes

1. B. Wiedenheft, S. H. Sternberg, J. A. Doudna, *Nature* **482**, 331 (2012).
2. D. Bhaya, M. Davison, R. Barrangou, *Annu. Rev. Genet.* **45**, 273 (2011).
3. M. P. Terns, R. M. Terns, *Curr. Opin. Microbiol.* **14**, 321 (2011).
4. M. Jinek *et al.*, *Science* **337**, 816 (2012).
5. G. Gasiunas, R. Barrangou, P. Horvath, V. Siksnys, *Proc. Natl. Acad. Sci. U.S.A.* **109**, E2579 (2012).
6. R. Sapranauskas *et al.*, *Nucleic Acids Res.* **39**, 9275 (2011).
7. T. R. Brummelkamp, R. Bernards, R. Agami, *Science* **296**, 550 (2002).
8. M. Miyagishi, K. Taira, *Nat. Biotechnol.* **20**, 497 (2002).
9. E. Deltcheva *et al.*, *Nature* **471**, 602 (2011).
10. J. Zou, P. Mali, X. Huang, S. N. Dowey, L. Cheng, *Blood* **118**, 4599 (2011).
11. N. E. Sanjana *et al.*, *Nat. Protoc.* **7**, 171 (2012).
12. J. H. Lee *et al.*, *PLoS Genet.* **5**, e1000718 (2009).
13. D. Hockemeyer *et al.*, *Nat. Biotechnol.* **27**, 851 (2009).
14. S. Kosuri *et al.*, *Nat. Biotechnol.* **28**, 1295 (2010).
15. V. Pattanayak, C. L. Ramirez, J. K. Joung, D. R. Liu, *Nat. Methods* **8**, 765 (2011).
16. N. M. King, O. Cohen-Haguenauer, *Mol. Ther.* **16**, 432 (2008).
17. Y. G. Kim, J. Cha, S. Chandrasegaran, *Proc. Natl. Acad. Sci. U.S.A.* **93**, 1156 (1996).
18. E. J. Rebar, C. O. Pabo, *Science* **263**, 671 (1994).
19. J. Boch *et al.*, *Science* **326**, 1509 (2009).
20. M. J. Moscou, A. J. Bogdanove, *Science* **326**, 1501 (2009).
21. L. Cong *et al.*, *Science* **339**, 819 (2013).
22. A. S. Khalil, J. J. Collins, *Nat. Rev. Genet.* **11**, 367 (2010).
23. P. E. Purnick, R. Weiss, *Nat. Rev. Mol. Cell Biol.* **10**, 410 (2009).
24. J. Zou *et al.*, *Cell Stem Cell* **5**, 97 (2009).
25. N. Holt *et al.*, *Nat. Biotechnol.* **28**, 839 (2010).
26. F. D. Urnov *et al.*, *Nature* **435**, 646 (2005).
27. A. Lombardo *et al.*, *Nat. Biotechnol.* **25**, 1298 (2007).
28. H. Li *et al.*, *Nature* **475**, 217 (2011).

Acknowledgments: This work was supported by NIH grant P50 HG005550. We thank S. Kosuri for advice on the oligonucleotide pool designs and synthesis. G.M.C. and P.M. have filed a patent based on the findings of this study.

Supplementary Materials

www.sciencemag.org/cgi/content/full/science.1232033/DC1
Materials and Methods
Supplementary Text
Figs. S1 to S11
Tables S1 to S3
References (*29*–*46*)

26 October 2012; accepted 12 December 2012
Published online 3 January 2013;
10.1126/science.1232033

Cyclic GMP-AMP Is an Endogenous Second Messenger in Innate Immune Signaling by Cytosolic DNA

Jiaxi Wu,[1]* Lijun Sun,[1,2]* Xiang Chen,[1] Fenghe Du,[1] Heping Shi,[3] Chuo Chen,[3] Zhijian J. Chen[1,2]†

Cytosolic DNA induces type I interferons and other cytokines that are important for antimicrobial defense but can also result in autoimmunity. This DNA signaling pathway requires the adaptor protein STING and the transcription factor IRF3, but the mechanism of DNA sensing is unclear. We found that mammalian cytosolic extracts synthesized cyclic guanosine monophosphate–adenosine monophosphate (cyclic GMP-AMP, or cGAMP) in vitro from adenosine triphosphate and guanosine triphosphate in the presence of DNA but not RNA. DNA transfection or DNA virus infection of mammalian cells also triggered cGAMP production. cGAMP bound to STING, leading to the activation of IRF3 and induction of interferon-β. Thus, cGAMP in metazoans and functions as an endogenous second messenger that triggers interferon production in response to cytosolic DNA.

Host defense against foreign genetic elements is one of the most fundamental functions of a living organism. The presence of self or foreign DNA in the cytoplasm is sensed by eukaryotic cells as a danger signal or a sign of foreign invasion (*1*). DNA can be introduced into the cytoplasm by bacterial or viral infection, transfection, or "leakage" from the nucleus or mitochondria under some pathological conditions that cause autoimmune diseases such as lupus. In mammalian cells, cytosolic DNA triggers the production of type I interferons and other cytokines through the endoplasmic reticulum protein STING (also known as MITA, MPYS, or ERIS) (*2*). STING recruits and activates the cytosolic kinases IKK and TBK1, which activate the transcription factors NF-κB and IRF3, respectively. NF-κB and IRF3 then enter the nucleus and function together to induce interferons and other cytokines. DNA-dependent RNA polymerase III has been shown to be a sensor that detects and transcribes AT-rich DNAs such as poly(deoxyadenosine-deoxythymidine) [poly(dA:dT)] into an RNA ligand capable of stimulating the RIG-I pathway to induce interferons (*3*, *4*). However, most DNA sequences do not activate the RNA polymerase III–RIG-I pathway. Instead, cytosolic DNA activates the STING-dependent pathway in a sequence-independent manner. How cytosolic DNA activates the STING pathway remains elusive.

We hypothesized that DNA binds to and activates a putative cytosolic DNA sensor, which then directly or indirectly activates STING, leading to the activation of IRF3 and NF-κB (fig. S1A). To test this model, we developed an in vitro complementation assay using the murine fibrosarcoma cell line L929, which is known to induce interferon-β (IFN-β) in a STING-dependent manner (*5*) (Fig. 1A). We used an L929 cell line stably expressing a short hairpin RNA (shRNA) against STING such that DNA transfection would only activate factors upstream of STING, including the putative DNA sensor (fig. S1, A and B). The L929-shSTING cells were transfected with different types of DNA, and then cytoplasmic extracts from these cells were mixed with the human monocytic cell line THP1 or murine macrophage cell line Raw264.7, which was permeabilized with perfringolysin O (PFO; Fig. 1A). PFO treatment pokes holes in the plasma membrane (*6*), allowing the cytoplasm to diffuse in and out of cells, while retaining organelles including the endoplasmic reticulum (which contains STING) and the Golgi apparatus inside the cells (*7*). If an upstream activator of STING is generated in the DNA-transfected cells, the cytoplasm containing such an activator is expected to activate STING in the PFO-permeabilized cells, leading to the phosphorylation and dimerization of IRF3.

Cytoplasmic extracts from L929-shSTING cells transfected with a DNA sequence known as interferon-stimulatory DNA (ISD; Fig. 1B, lane 2), poly(dA:dT), a GC-rich 50–base pair

[1]Department of Molecular Biology, University of Texas Southwestern Medical Center, Dallas, TX 75390, USA. [2]Howard Hughes Medical Institute, University of Texas Southwestern Medical Center, Dallas, TX 75390, USA. [3]Department of Biochemistry, University of Texas Southwestern Medical Center, Dallas, TX 75390, USA.

*These authors contributed equally to this work.
†To whom correspondence should be addressed. E-mail: zhijian.chen@utsouthwestern.edu

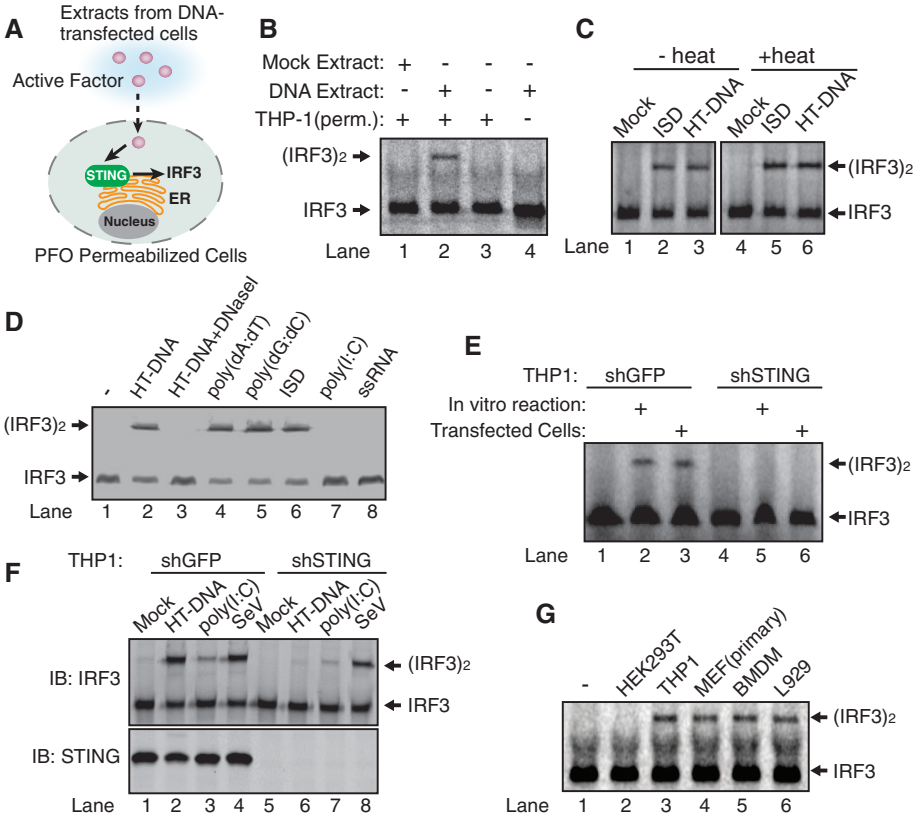

Fig. 1. DNA-dependent generation of a heat-resistant small molecule activates the STING pathway. (**A**) Illustration of an activity assay for cellular factors that activate the STING pathway. (**B**) Cytosolic extracts from mock or ISD-transfected L929-shSTING cells were incubated with PFO-permeabilized THP1 cells together with ^{35}S-labeled IRF3. Dimerization of IRF3 was analyzed by native gel electrophoresis followed by autoradiography. (**C**) Similar to (B), except that in lanes 4 to 6, cytosolic extracts were heated at 95°C for 5 min to denature proteins and then the heat-resistant supernatant was incubated with PFO-permeabilized THP1 cells. (**D**) L929-shSTING cytosolic extracts were incubated with the indicated nucleic acids in the presence of ATP, and then the heat-resistant supernatant was assayed for its ability to stimulate IRF3 dimerization in permeabilized Raw264.7 cells. (**E**) THP1 cells stably expressing shRNA against GFP (control) or STING were permeabilized with PFO and then incubated with the heat-resistant supernatant from the reaction mixture containing DNA-supplemented L929 cytosolic extracts (lanes 2 and 5) or from DNA-transfected L929 cells (lanes 3 and 6). IRF3 activation was analyzed by native gel electrophoresis. (**F**) THP1 cells described in (E) were transfected with HT-DNA or poly(I:C) or infected with Sendai virus (SeV), followed by measurement of IRF3 dimerization. (**G**) Cytosolic extracts from the indicated cell lines were incubated with HT-DNA, and then heat-resistant supernatants were assayed for their ability to stimulate IRF3 dimerization in permeabilized Raw264.7 cells. Unless noted otherwise, all results in this and other figures were representative of at least two independent experiments.

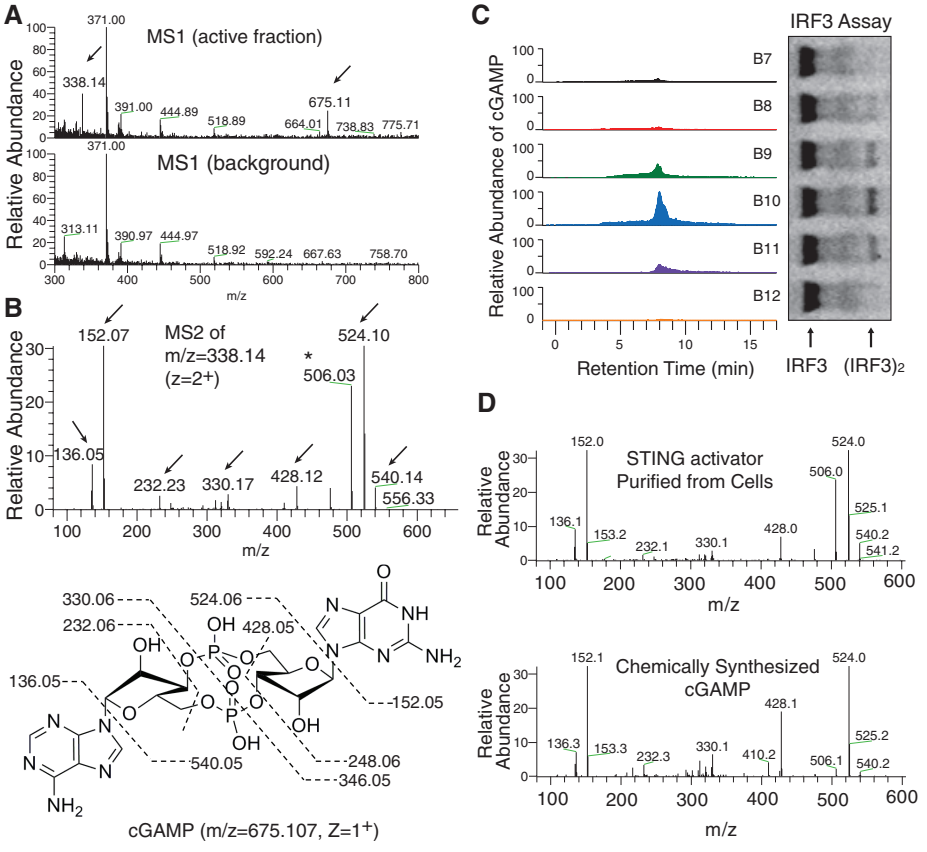

Fig. 2. Purification and identification of the heat-resistant STING activator. (**A**) Full scan nano-LC-MS spectra of active and inactive fractions from the C18 column. Arrows indicate an ion at +1 (675.11) and +2 (338.14) charge states present only in the active fraction. (**B**) Tandem mass (MS2) spectra after CID fragmentation of the ion with m/z = 338.14 (z = 2) from the MS1 scan shown in (A). Arrows indicate the m/z values of the expected fragmentation patterns of cyclic GMP-AMP (cGAMP, bottom). Asterisk indicates an ion (m/z = 506) that resulted from a neutral loss of a water molecule (18) from the ion with m/z = 524. (**C**) Fractions (B7 to B12) from the C18 column were analyzed for the presence of cGAMP by selective reaction monitoring of the expected ions and for their ability to stimulate IRF3 dimerization. (**D**) Comparison of the CID MS2 spectra of the purified STING activator and chemically synthesized cGAMP.

double-stranded DNA (G:C50), poly(deoxyinosine-deoxycytidine) [poly(dI:dC)], or herring testis DNA (HT-DNA; fig. S1C) activated IRF3 in permeabilized THP1 cells, indicating that this activity was independent of DNA sequence. To determine whether the STING activator is a protein, we incubated the cytoplasmic extracts at 95°C to denature most proteins and then incubated the "heat supernatant" with permeabilized THP1 cells. Surprisingly, the heat supernatant from the ISD-transfected or HT-DNA–transfected cells caused IRF3 dimerization (Fig. 1C). This activity was resistant to treatment with Benzonase (Novagen, fig. S1D), which degrades both DNA and RNA, or proteinase K (fig. S1D). Thus, the STING activator is probably not a protein, DNA, or RNA.

To test whether DNA could stimulate the generation of the heat-resistant STING activator in vitro, we incubated HT-DNA with L929-shSTING cytoplasmic extracts (S100) in the presence of ATP (fig. S1E). The reaction mixture was heated at 95°C to denature proteins. Remarkably, incubation of the supernatant with permeabilized Raw264.7 cells led to IRF3 dimerization (Fig. 1D, lane 2). This activity depended on the addition of DNA to the cytoplasmic extracts. Other DNAs, including poly(dA:dT), poly(deoxyguanosine-deoxycytidine), and ISD, also stimulated the generation of the STING activator in L929-shSTING cytoplasmic extracts, whereas poly(inosine-cytidine) [poly(I:C)] and single-stranded RNA had no activity (Fig. 1D). Similar results were obtained with permeabilized THP1 cells (fig. S1F). Knockdown of STING in the permeabilized THP1 cells abolished IRF3 activation by the heat-resistant factor generated by DNA transfected into L929 cells or DNA added to L929 cytosolic extracts (Fig. 1E). Control experiments showed that the knockdown of STING inhibited the activation of IRF3 and induction of IFN-β and tumor necrosis factor–α in THP1 cells by HT-DNA transfection (fig. S1, G and H), but IRF3 activation by poly(I:C) transfection or Sendai virus infection, which is known to activate the RIG-I pathway, was unaffected by the STING knockdown (Fig. 1F). We also tested cytoplasmic extracts from several cell lines for their ability to produce the heat-resistant STING activator (Fig. 1G). Incubation of HT-DNA with extracts from primary mouse embryo fibroblasts (MEFs), mouse bone marrow–derived macrophages (BMDMs), and L929 cells led to generation of the heat-resistant factor that activated IRF3. Human cell extracts from THP1, but not human embryonic kidney (HEK) 293T cells, were also able to produce this STING activator. These results are in agreement with our previous finding that primary MEFs, BMDMs, and L929 and THP1 cells, but not HEK293T cells, possessed the STING-dependent, RNA polymerase III–independent, pathway to induce type I interferons (*3*).

We next used several chromatographic steps, including a STING-Flag affinity purification step, to purify the heat-resistant STING activator from L929 cell extracts (fig. S2, A and B). Previous research has shown that the bacterial molecules cyclic diadenylate monophosphate (c-di-AMP) and cyclic diguanylate monophosphate (c-di-GMP) bind to STING and induce type I interferons (*8*, *9*). However, using nano–liquid chromatography–mass spectrometry (nano-LC-MS), we did not detect MS or MS/MS spectra consistent with those expected of c-di-GMP ($[M+H]^+ = 691$) or c-di-AMP ($[M+H]^+ = 659$). In-depth examination

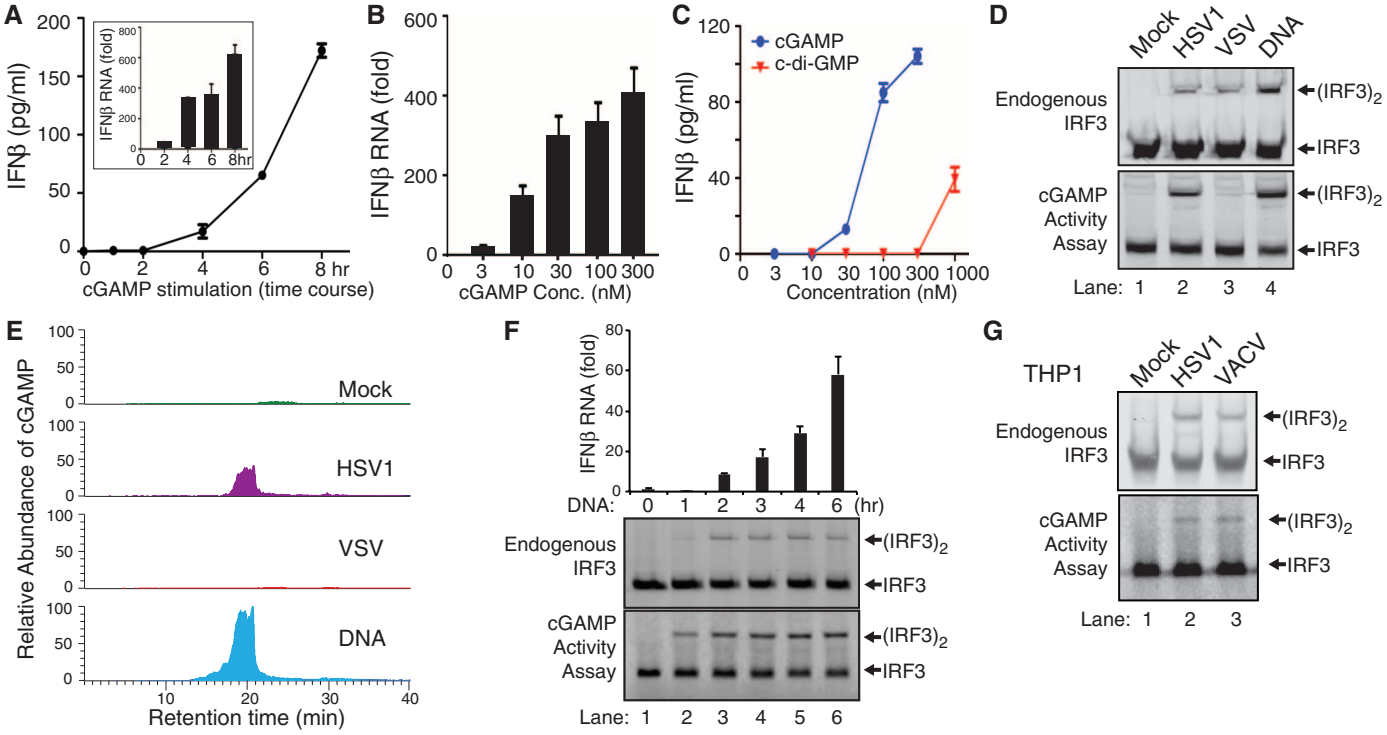

Fig. 3. DNA transfection and DNA virus infection induce IFN-β through cGAMP. (**A**) Chemically synthesized cGAMP (100 nM) was delivered to digitonin-permeabilized L929 cells for the indicated times, then IFN-β RNA and secreted protein were measured by qRT-PCR (inset) and ELISA, respectively. Unless noted otherwise, the error bars in this and all other panels denote SEM ($n = 3$). (**B**) Similar to (A), except that different concentrations of cGAMP were delivered into L929 cells for 8 hours, followed by qRT-PCR analyses of IFN-β RNA. (**C**) Similar to (B), except that different concentrations of cGAMP and c-di-GMP were delivered into L929 cells, followed by ELISA assays for IFN-β. (**D**) L929 cells were infected with HSV-1Δ34.5 or VSV-ΔM51-GFP, transfected with HT-DNA, or mock-treated. An aliquot of the cell extracts was directly analyzed for IRF3 dimerization (top), whereas another aliquot was heated to denature proteins and the heat-resistant supernatant was assayed for its ability to stimulate IRF3 dimerization in permeabilized Raw264.7 cells (bottom). (**E**) The heat-resistant supernatant from (D) was fractionated by HPLC using a C18 column, and the presence of cGAMP in the fractions was measured by mass spectrometry using SRM. (**F**) L929 cells were transfected with HT-DNA (4 μg/ml) for the indicated time, then IFN-β RNA was measured by qRT-PCR and IRF3 dimerization was analyzed by native polyacrylamide gel electrophoresis (PAGE). Aliquots of the cell extracts were tested for the presence of cGAMP on the basis of its ability to induce IRF3 dimerization after delivery into Raw264.7 cells. (**G**) THP1 cells were infected with HSV-1Δ34.5 and vaccinia virus (VACV) for 6 hours, then the activation of endogenous IRF3 and generation of cGAMP activity were measured as described in (F).

of the MS spectra revealed two ions with mass-to-charge ratios (*m/z*) of 675.1 ($z = 1^+$) and 338.1 ($z = 2^+$), which were present in the active fractions but absent in the background spectra (Fig. 2A). These *m/z* values, despite the low mass accuracy of the mass spectrometer (LTQ, Thermo), were equivalent to the average calculated *m/z* values of c-di-GMP and c-di-AMP [675 = (691 + 659)/2]. This observation suggested that the detected ion was a hybrid of c-di-GMP and c-di-AMP—that is, cyclic GMP-AMP, or cGAMP (*m/z* = 675.107, $z = 1^+$; *m/z* = 338.057, $z = 2^+$). Collision-induced dissociation (CID) fragmentation of this ion (*m/z* = 338.1, $z = 2^+$) revealed several prominent ions with *m/z* values expected of the product ions of cGAMP (Fig. 2B). Quantitative mass spectrometry using selective reaction monitoring (SRM) showed that the abundance of the ions representing cGAMP in the fractions from a C18 column correlated very well with their IRF3-stimulatory activities (Fig. 2C and fig. S2C). cGAMP has recently been identified in the bacterium *Vibrio cholerae* and shown to play a role in bacterial chemotaxis and colonization (*10*). However, cGAMP has not been reported to exist or function in eukaryotic cells.

To verify the identity of the heat-resistant STING activator, we used a high-resolution high-accuracy mass spectrometer (Q Exactive, Thermo) to perform nano-LC-MS analysis. The cell-derived STING activator had *m/z* values of 675.107 ($z = 1^+$) and 338.057 ($z = 2^+$), which exactly matched the theoretical values of cGAMP (fig. S2D). To further characterize the structure and function of cGAMP, we developed a 10-step single-flask protocol to chemically synthesize cGAMP (fig. S3). The MS/MS spectra of the cell-derived STING activator were identical to those of the chemically synthesized cGAMP (Fig. 2D). These results demonstrate that L929 cells produced cGAMP.

Quantitative reverse transcription polymerase chain reaction (qRT-PCR) and enzyme-linked immunosorbent assay (ELISA) showed that chemically synthesized cGAMP induced IFN-β RNA and protein in L929 cells after introduction into the cells (Fig. 3A). Titration experiments showed that cGAMP induced IFN-β RNA robustly even at concentrations as low as 10 nM (Fig. 3B). Indeed, ELISA indicated that cGAMP was much more potent than c-di-GMP in inducing IFN-β (Fig. 3C). cGAMP was also more potent than c-di-GMP and c-di-AMP in activating IRF3 (fig. S4A). To determine whether L929 extracts contained enzymes that could synthesize other types of dinucleotides or oligonucleotides capable of activating IRF3, we tested all four ribonucleotides in various combinations (fig. S4B). ATP and GTP were both necessary and sufficient to support the synthesis of an activator of IRF3, further supporting the idea that L929 cells contain an enzyme that synthesizes cGAMP from ATP and GTP.

To determine whether DNA virus infection leads to the production of cGAMP in cells, we infected L929 cells with HSV-1 lacking ICP34.5, a viral protein known to antagonize interferon production in the infected cells (*11*). Like DNA transfection, HSV-1ΔICP34.5 infection led to IRF3 activation in L929 cells (Fig. 3D, upper). Cell extracts from the DNA-transfected or virus-infected cells contained a heat-resistant factor that could activate IRF3 in permeabilized Raw264.7 cells (Fig. 3D, lower panel). As a control, we infected L929 cells with a vesicular stomatitis virus strain, VSV = ΔM51 [fused to green fluorescent protein (VSV-ΔM51-GFP)], an RNA virus known to trigger strong interferon production through the RIG-I pathway (*12*, *13*). In contrast to HSV-1, VSV-infected cells did not contain the heat-resistant IRF3 activator in the same in vitro assay, although VSV infection did induce IRF3 activation in L929 cells (Fig. 3D). The heat-resistant factor in HSV-1–infected cells was enriched by reversed-phase high-performance liquid chromatography (HPLC) and quantified by nano-LC-MS using SRM. DNA-transfected or HSV-1–infected cells, but not mock-treated or VSV-infected cells, produced elevated levels of cGAMP (Fig. 3E). Kinetic experiments showed that after DNA was transfected into L929 cells, cGAMP was produced before IRF3 dimerization and IFN-β induction could be detected (Fig. 3F). To test whether DNA viruses could induce cGAMP production in human cells, we infected THP1 cells with HSV1 or vaccinia virus (VACV; Fig. 3G). Both viruses induced IRF3 dimerization

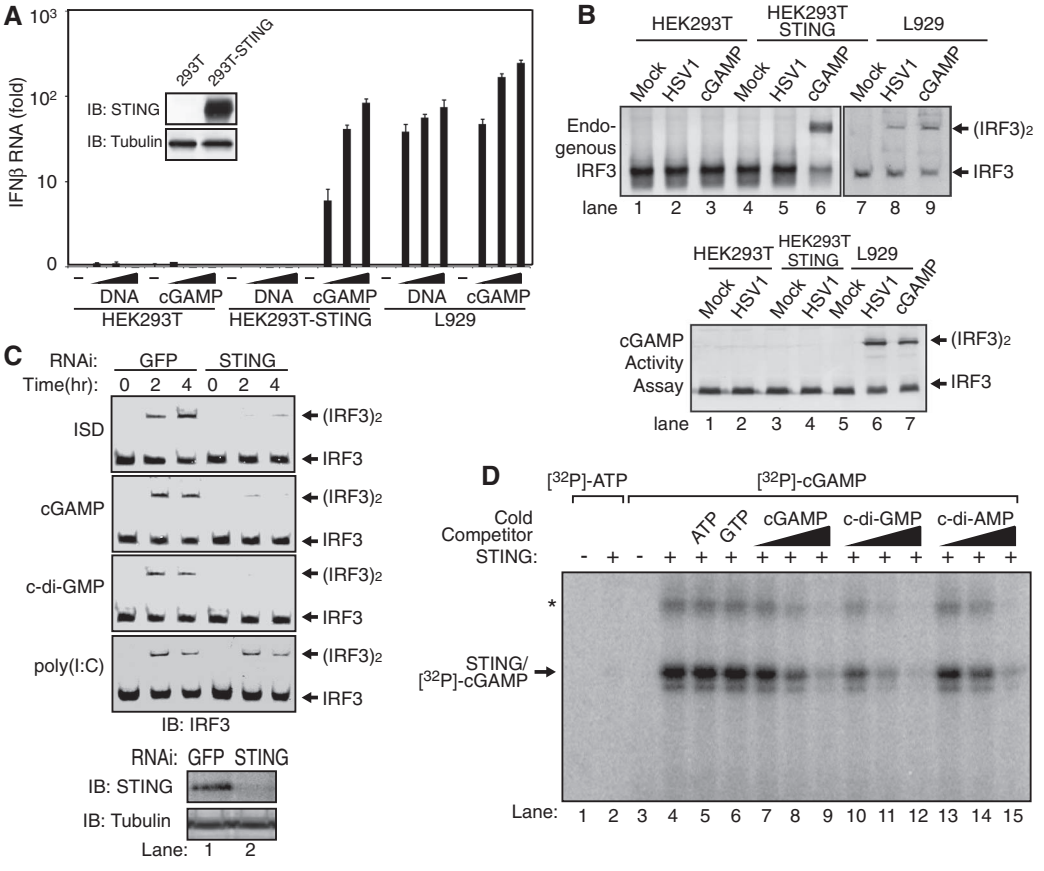

Fig. 4. cGAMP binds to STING and activates IRF3 in a STING-dependent manner. (**A**) Increasing concentrations of HT-DNA or cGAMP were delivered to indicated cells, and the induction of IFN-β was measured by qRT-PCR. Inset shows immunoblots of STING and β-tubulin in the cell lines. (**B**) Indicated cell lines were infected with HSV1Δ34.5 or permeabilized with digitonin and then incubated with cGAMP. Activation of endogenous IRF3 was analyzed by native gel electrophoresis (top). Aliquots of the cytosolic extracts were heated to denature proteins, and the supernatant was assayed for its ability to stimulate IRF3 in permeabilized Raw264.7 cells (bottom). (**C**) cGAMP, c-di-GMP, ISD, or poly(I:C) was delivered into L929 cells stably expressing a shRNA against GFP or STING for the indicated time, followed by analysis of IRF3 dimerization. (**D**) Recombinant STING protein was incubated with [^{32}P]ATP or [^{32}P]cGAMP in the presence or absence of the cold competitors as indicated. After UV cross-linking, the mixtures were resolved by SDS-PAGE followed by autoradiography.

in the cells, and both viruses also triggered the production of cGAMP that activated IRF3 (Fig. 3G, lower panel). Collectively, these results indicate that DNA transfection and DNA virus infections in human and mouse cells produced cGAMP, which led to IRF3 activation.

To determine whether cGAMP activates IRF3 through STING, we carried out three sets of experiments. First, we established a HEK293T cell line stably expressing STING, stimulated these cells with cGAMP, and then measured IFN-β induction by quantitative RT-PCR (Fig. 4A). HEK293T cells did not respond to cGAMP, likely because of absent or very low STING expression in these cells. The expression of STING in HEK293T cells rendered a high level of IFN-β induction by cGAMP. However, DNA did not stimulate HEK293T-STING cells to induce IFN-β, consistent with a defect of HEK293T cells in producing cGAMP in response to DNA stimulation. In contrast, L929 cells induced IFN-β in response to stimulation by either cGAMP or DNA. HSV-1 infection induced IRF3 dimerization in L929 cells but not in HEK293T or HEK293T-STING cells (Fig. 4B, upper panel), which suggests that the production of cGAMP is important for HSV-1 to activate IRF3 in cells. Indeed, extracts from HSV1-infected L929 cells, but not from HEK293T or HEK293T-STING cells, contained the cGAMP activity that led to IRF3 dimerization in permeabilized Raw264.7 cells (Fig. 4B, lower panel). These results indicate that the expression of STING in HEK293T cells installed the ability of the cells to activate IRF3 and induce IFN-β in response to cGAMP, but was insufficient to install the response to DNA or DNA viruses because of a defect of HEK293T cells in synthesizing cGAMP.

Second, we tested the response of L929 and L929-shSTING cells to cGAMP (Fig. 4C). Similar to ISD and c-di-GMP, cGAMP-induced IRF3 dimerization was dependent on STING. In contrast, poly(I:C) still induced IRF3 dimerization in the absence of STING. These results demonstrate that STING is necessary for cGAMP to activate IRF3.

Finally, we examined whether STING binds to cGAMP directly. Recombinant STING protein containing residues 139 to 379, which has been shown to bind c-di-GMP (*14*), was expressed and purified from *Escherichia coli* and then incubated with [^{32}P]cGAMP followed by ultraviolet (UV)–induced cross-linking (Fig. 4D). A radiolabeled band corresponding to a cross-linked STING-cGAMP complex was detected when both STING and [^{32}P]cGAMP were present. High concentrations of ATP or GTP did not compete with the formation of the STING-cGAMP complex. By contrast, the intensity of this band decreased as the concentrations of competing cold cGAMP, c-di-GMP, or c-di-AMP increased; this finding suggests that the cGAMP binding sites on STING might overlap with those that interact with c-di-GMP and c-di-AMP. Indeed, mutations of several residues that were recently shown to participate in the binding of STING to c-di-GMP (*14*), including Ser^{161} → Tyr, Tyr^{240} → Ser, and Asn^{242} → Ala, also impaired the binding of STING to cGAMP (fig. S5). Collectively, these results demonstrate that cGAMP is a ligand that binds to and activates STING.

Cyclic dinucleotides have been shown to function as bacterial second messengers that regulate a variety of physiological processes, including bacterial motility and biofilm formation (*15*). A recent report showed that c-di-GMP is produced in the protozoan *Dictyostelium* and functions as a morphogen to induce stalk cell differentiation (*16*). Our results identify cGAMP as a first cyclic dinucleotide in metazoa and show that cGAMP is a potent inducer of type I interferons. The role of cGAMP is similar to that of cyclic adenosine monophosphate (cAMP), the best-studied second messenger (*17*). Like cAMP, which is synthesized by adenylate cyclase upon its activation by upstream ligands, cGAMP is synthesized by a cyclase in response to stimulation by a DNA ligand (*18*). cAMP binds to and activates protein kinase A and other effector molecules. Similarly, cGAMP binds to and activates STING to trigger the downstream signaling cascades. As an endogenous molecule in mammalian cells, cGAMP may be used in immune therapy or as a vaccine adjuvant.

References and Notes

1. R. Barbalat, S. E. Ewald, M. L. Mouchess, G. M. Barton, *Annu. Rev. Immunol.* **29**, 185 (2011).
2. G. N. Barber, *Immunol. Rev.* **243**, 99 (2011).
3. Y. H. Chiu, J. B. Macmillan, Z. J. Chen, *Cell* **138**, 576 (2009).
4. A. Ablasser *et al.*, *Nat. Immunol.* **10**, 1065 (2009).
5. Y. Tanaka, Z. J. Chen, *Sci. Signal.* **5**, ra20 (2012).
6. J. Rossjohn *et al.*, *J. Mol. Biol.* **367**, 1227 (2007).
7. T. Saitoh *et al.*, *Proc. Natl. Acad. Sci. U.S.A.* **106**, 20842 (2009).
8. J. J. Woodward, A. T. Iavarone, D. A. Portnoy, *Science* **328**, 1703 (2010).
9. D. L. Burdette *et al.*, *Nature* **478**, 515 (2011).
10. B. W. Davies, R. W. Bogard, T. S. Young, J. J. Mekalanos, *Cell* **149**, 358 (2012).
11. K. L. Mossman, J. R. Smiley, *J. Virol.* **76**, 1995 (2002).
12. D. F. Stojdl *et al.*, *Cancer Cell* **4**, 263 (2003).
13. Q. Sun *et al.*, *Immunity* **24**, 633 (2006).
14. Q. Yin *et al.*, *Mol. Cell* **46**, 735 (2012).
15. C. Pesavento, R. Hengge, *Curr. Opin. Microbiol.* **12**, 170 (2009).
16. Z. H. Chen, P. Schaap, *Nature* **488**, 680 (2012).
17. S. A. Blumenthal, *Perspect. Biol. Med.* **55**, 236 (2012).
18. L. Sun, J. Wu, F. Du, X. Chen, Z. J. Chen, *Science* 10.1126/science.1232458 (2012).

Acknowledgments: We thank Y. Tanaka for generating HEK293T-STING and L929-shSTING cell lines; J. Bell, B. Levine, and L. Deng for VSV, HSV-1, and VACV, respectively; R. Debose-Boyd for the PFO plasmid; and V. Sperandio for *V. cholerae* strain C6709. Supported by NIH grants AI-093967 (Z.J.C.) and GM-079554 (C.C.). Z.J.C. is an investigator of Howard Hughes Medical Institute.

Supplementary Materials

www.sciencemag.org/cgi/content/full/science.1229963/DC1
Materials and Methods
Table S1
Figs. S1 to S5
References (*19*, *20*)

10 September 2012; accepted 11 December 2012
Published online 20 December 2012;
10.1126/science.1229963

Prediction Error Governs Pharmacologically Induced Amnesia for Learned Fear

Dieuwke Sevenster,[1,2] Tom Beckers,[1,2,3] Merel Kindt[1,2]*

Although reconsolidation opens up new avenues to erase excessive fear memory, subtle boundary conditions put constraints on retrieval-induced plasticity. Reconsolidation may only take place when memory reactivation involves an experience that engages new learning (prediction error). Thus far, it has not been possible to determine the optimal degree of novelty required for destabilizing the memory. The occurrence of prediction error could only be inferred from the observation of a reconsolidation process itself. Here, we provide a noninvasive index of memory destabilization that is independent from the occurrence of reconsolidation. Using this index, we show in humans that prediction error is (i) a necessary condition for reconsolidation of associative fear memory and (ii) determined by the interaction between original learning and retrieval. Insight into the process of memory updating is crucial for understanding the optimal and boundary conditions on reconsolidation and provides a clear guide for the development of reconsolidation-based treatments.

A consolidated fear memory can enter a transient labile phase upon its reactivation. Pharmacological blockade of the subsequent protein synthesis–dependent restabilization (reconsolidation) produces a memory deficit in both animals (*1*) and humans (*2*). However, an independent measure for memory destabilization other than the occurrence of reconsolidation itself is not yet available. The functional role of reconsolidation might be to keep